



# HHS Public Access

Author manuscript

*Neuroimage*. Author manuscript; available in PMC 2017 May 01.

Published in final edited form as:

*Neuroimage*. 2016 May 1; 131: 126–132. doi:10.1016/j.neuroimage.2015.05.063.

## Cardiorespiratory Fitness Modifies the Relationship between Myocardial Function and Cerebral Blood Flow in Older Adults

Nathan F. Johnson<sup>a</sup>, Brian T. Gold<sup>b,c,d</sup>, Alison L. Bailey<sup>e</sup>, Jody L. Clasey<sup>f,g</sup>, Jonathan G. Hakun<sup>b</sup>, Matthew White<sup>e,1</sup>, Doug Long<sup>g,h</sup>, and David K. Powell<sup>b,c</sup>

<sup>a</sup> Department of Rehabilitation Sciences, Division of Physical Therapy, University of Kentucky, Lexington, KY 40536, USA

<sup>b</sup> Department of Anatomy and Neurobiology, University of Kentucky, Lexington, KY 40536, USA

<sup>c</sup> Magnetic Resonance Imaging and Spectroscopy Center, University of Kentucky, Lexington, KY 40536, USA

<sup>d</sup> Sanders-Brown Center on Aging, University of Kentucky, Lexington, KY 40536, USA

<sup>e</sup> Gill Heart Institute, University of Kentucky, Lexington, KY 40536, USA

<sup>f</sup> Department of Kinesiology and Health Promotion, University of Kentucky, Lexington, KY 40536, USA

<sup>g</sup> Clinical Services Core, University of Kentucky, Lexington, KY 40536, USA

<sup>h</sup> College of Health Sciences, University of Kentucky, Lexington, KY 40536, USA

### Abstract

A growing body of evidence indicates that cardiorespiratory fitness attenuates some age-related cerebral declines. However, little is known about the role that myocardial function plays in this relationship. Brain regions with high resting metabolic rates, such as the default mode network (DMN), may be especially vulnerable to age-related declines in myocardial functions affecting cerebral blood flow (CBF). This study explored the relationship between a measure of myocardial mechanics, global longitudinal strain (GLS), and CBF to the DMN. In addition, we explored how cardiorespiratory affects this relationship. Participants were 30 older adults between the ages of 59 and 69 (mean age = 63.73 years, SD = 2.8). Results indicated that superior cardiorespiratory fitness and myocardial mechanics were positively associated with DMN CBF. Moreover, results of a mediation analysis revealed that the relationship between GLS and DMN CBF was accounted for by individual differences in fitness. Findings suggest that benefits of healthy heart function to brain function are modified by fitness.

---

Correspondence: Nathan F. Johnson, Department of Rehabilitation Sciences Division of Physical Therapy, University of Kentucky College of Health Sciences, Lexington, KY, 40536-0298, Phone: (859) 218—5429, Fax: (859) 257-6700, nathan.johnson@uky.edu, brian.gold@uky.edu, jghakun@uky.edu, dkpove00@mri.uky.edu, alison.bailey@uky.edu, matt.white@uky.edu, jlclas0@email.uky.edu, delong2@uky.edu

<sup>1</sup>Present Address: WakeMed Physician Practices, Raleigh, NC 27610, USA

**Publisher's Disclaimer:** This is a PDF file of an unedited manuscript that has been accepted for publication. As a service to our customers we are providing this early version of the manuscript. The manuscript will undergo copyediting, typesetting, and review of the resulting proof before it is published in its final citable form. Please note that during the production process errors may be discovered which could affect the content, and all legal disclaimers that apply to the journal pertain.

## Keywords

aging; arterial spin labeling; cardiorespiratory fitness; default mode network; global longitudinal strain

---

## INTRODUCTION

Growing evidence suggests that physical activity and exercise have protective effects on brain health (Kramer and Erickson, 2007; Smith et al., 2010). Animal models suggest that cardiorespiratory fitness (fitness<sub>CR</sub>) may benefit brain health in part via vascular changes that increase cerebral blood flow, CBF (Swain et al., 2003). However, less is known about the relationship between fitness<sub>CR</sub> and CBF in humans and how these measures are linked to myocardial function. Global longitudinal strain (GLS), a measure associated with left ventricular myocardial tissue deformation (Hoit, 2011; Reisner et al., 2004), is a strong indicator of myocardial function and is associated with subclinical brain disease in the absence of cardiac disease (Russo et al., 2013). Thus, the predictive power of GLS makes it an ideal proxy of cardiac function when attempting to better understand the relationship between heart health and brain health in older adults.

To date, no study has explored the potential separate and joint contributions of fitness<sub>CR</sub> and myocardial function to brain CBF. The default mode network (DMN) is a set of intrinsically connected regions that are most active when not specifically engaged in an externally directed cognitive task (Buckner et al., 2008; Buckner and Carroll, 2007; Dixon et al., 2014). The DMN includes the medial prefrontal cortex (mPFC), anterior and posterior cingulate cortex (ACC/PCC), and medial temporal cortex, regions that show disproportionately high resting metabolic rates (Buckner et al., 2008; Gusnard and Raichle, 2001) and susceptibility to healthy aging and Alzheimer's disease (Buckner et al., 2005; Koch et al., 2010). The DMN is therefore an ideal target to determine these relationships using ASL-MRI.

In the present study, we explored the relationship between fitness<sub>CR</sub> and CBF to the DMN using an independent component analysis (ICA) to identify the DMN in an unbiased manner. In addition, we explored the role of myocardial function in CBF to the DMN. Declines in cardiac function are associated with accelerated brain aging (Jefferson et al., 2010) and precede disease processes characterized by declines in cognitive function, such as Alzheimer's disease (de la Torre, 2009; de la Torre, 2010). However, training-induced increases in fitness<sub>CR</sub> are associated with augmented maximal cardiac output and not resting cardiac output (Ehsani et al., 1991; Stratton et al., 1994), suggesting that improving fitness<sub>CR</sub> through regular physical activity may help to protect the brain from age-related declines in resting cardiac function.

## METHODS

### Participants

Forty-two community dwelling healthy volunteers (14 males) participated in this study (mean age = 63.89 years, SD = 2.94). Participants provided written informed consent in a manner approved by the University of Kentucky Institutional Review Board and were

monetarily rewarded for participating. Twelve of these 42 participants (5 male) were excluded from the study. Of these twelve participants five did not complete the treadmill test because they were either currently taking a beta-blocker, they reported a history of cardiac ablation, or the supervising cardiologist terminated the test due to an abnormal electrocardiogram (ECG). One participant voluntarily terminated the test due to mouthpiece discomfort and another participant was unable to complete the MRI scan due to the presence of a scleral buckle. The remaining 5 participants were excluded because they failed to achieve  $\text{VO}_2$  peak (described below).

The 30 remaining participants (9 males) ranged in age from 59 to 69 (mean age = 63.73 years,  $\text{SD} = 2.8$ ). Participants met all criteria for participating in a magnetic resonance imaging (MRI) study. Exclusion for the MRI study included history of a major head injury and/or concussion, neurological disorder (e.g., stroke, seizure), or the presence of metal fragments and/or metallic implants that could cause bodily injury or disrupt the magnetic field. All participants also met all criteria for participating in a maximal graded exercise test. Exclusion for the graded exercise test included a diagnosis of any major medical condition (e.g., heart, lung, or kidney disease), a history of uncontrolled high blood pressure, uncontrolled diabetes, a history of heart complications (e.g., heart murmur or coronary artery disease), pulmonary dysfunction (e.g., severe asthma, chronic obstructive pulmonary disease, emphysema), or orthopedic limitations (e.g., foot, knee, or hip problems) that would result in bodily injury or limit performance. A modified version of the Physical Activity Readiness Questionnaire (PAR-Q) was used to screen participants prior to participation in the study. Additionally, physician clearance was obtained for each participant.

### **Echocardiography**

A limited study transthoracic echocardiogram was obtained on each participant adhering to American Society of Echocardiography (ASE) criteria (Mor-Avi et al., 2011). Echocardiography was performed with a commercially available scanner (IE33, Phillips) and transducer. Imaging data was acquired by two level 2 echo trained cardiovascular physicians who were part of the study team. Several consecutive cardiac cycles were stored for later post-processing on an external workstation by the same two physicians. Two-dimensional global longitudinal strain (speckle-tracking) was calculated using dedicated software (QLAB, Phillips). Since GLS quantifies left ventricular myocardial shortening during systole, lower more negative values represent superior myocardial mechanics. Lastly, to render GLS-CBF and GLS-fitness<sub>CR</sub> relationships more interpretable, participant's GLS values were multiplied by  $-1$  so that higher scores reflect superior myocardial shortening mechanics.

### **Cardiorespiratory Fitness Assessment**

All participants completed a physician-supervised maximal graded exercise test (Max GXT) to assess  $\text{VO}_2$  peak using a previously described standardized protocol (Johnson et al., 2012). Briefly, the exercise test was conducted in the Assessment Laboratory of the University of Kentucky's Center for Clinical and Translational Sciences Translation Analytic and Assessment Core using an indirect calorimetry system with integrated 12-lead ECG

(Sensormedics Vmax229 metabolic cart; Yorba Linda, CA). A multistage stepwise treadmill protocol, including 3-minute stages, was used to assess fitness<sub>CR</sub>.

During the Max GXT continuous heart rate and dynamic heart function were measured and monitored via 12-lead ECG. Oxygen consumption was measured breath-by-breath and later averaged over one minute intervals and expressed relative to body weight (ml/kg/min) during the test and recovery period. Manual blood pressures and rating of perceived exertion (RPE; using the modified Borg Scales) were collected during the final 30 sec of each 3-minute stage. All tests were terminated upon participant reported volitional fatigue, the presence of any absolute or relative indications for terminating exercise testing in accordance with the American College of Sports Medicine's Guidelines for Exercise Testing and Prescription (Thompson et al., 2010), or any symptom the supervising physician considered hazardous to the well-being of the participant. All exercise tests were performed within 23 days of the acquisition of the MRI (mean = 10.4, SD = 4.9).

VO<sub>2</sub> peak was defined as meeting 2 of the following 3 criteria: 1) achievement of an age-predicted maximum HR; 2) self-reported RPE scores  $\geq 17$ ; and 3) a respiratory exchange ratio of  $\geq 1.1$ . Additionally, the highest observed VO<sub>2</sub> value was used for all analyses. The standard 220-age equation was used to calculate age-predicted maximum HR. Five participants were not included in the analysis because they failed to meet 2 of the 3 criteria.

The primary purpose of the study was to characterize the relationship between myocardial function, fitness<sub>CR</sub>, and cerebral blood flow. We used a modified version of our previously constructed composite score (see Johnson et al., 2012) which includes total time on treadmill (seconds) and VO<sub>2</sub> peak, two fitness<sub>CR</sub> metrics shown to be predictive of WM microstructure (Johnson et al., 2012), to generate a score representative of fitness<sub>CR</sub>. Briefly, values for VO<sub>2</sub> peak and total time on treadmill were normalized across each aerobic fitness<sub>CR</sub> metric [e.g., normalized value  $A = (A - \text{min}) / (\text{max} - \text{min})$ ; range from 0 to 1 for each metric] and then summed to create a single value between 0 and 2 (i.e., composite-fitness<sub>CR</sub>). Values closer to 0 represent those participants with lower fitness<sub>CR</sub> levels and values closer to 2 represent those participants with higher fitness<sub>CR</sub> levels.

### MRI Acquisition

Data were collected on a 3 Tesla Siemens TIM scanner at the University of Kentucky. A 32-channel imaging coil was used. Three primary imaging sequences were collected for each participant in this study: 1) a high-resolution, T1-weighted sequence for subsequent localization of cerebral blood flow and resting-state activity in standard stereotactic space; 2) T2\*-weighted images sensitive to resting fluctuations in BOLD signal; and 3) a Pulsed ASL (PASL) sequence for estimation of absolute cerebral blood flow.

Two high-resolution, 3D anatomic images were acquired using a magnetization-prepared rapid gradient-echo (MPRAGE) sequence with the following parameters: echo time (TE) 2.26 ms, repetition time (TR) 2530 ms, field of view (FOV) of 256 mm, flip angle (FA) of 7°, and voxel size of 1×1×1 mm. CBF was estimated using a PASL sequence with a proximal inversion with a control for off-resonance effects (PICORE) and quantitative

imaging of perfusion with a single subtraction and thin-slice  $T_{11}$  (700 ms) periodic saturation (Q2TIPS) sequence. One hundred and four images were acquired with  $T_{12} = 1900$  ms, TE = 12 ms, TR = 3400 ms, FA =  $90^\circ$ , FOV = 256 mm,  $64 \times 64$  matrix, and voxel size of  $4.0 \times 4.0 \times 5.0$  mm. Tag and untagged image pairs were acquired in order to calculate CBF in each voxel. A single M0 image was also acquired (total images collected = 105) prior to steady state. Finally,  $T_2^*$ -weighted images sensitive to changes in BOLD were acquired with the following parameters: TE 30 ms, TR 2000 ms, FOV = 224 mm, (FA) of  $76^\circ$ , and voxel size of  $3.5^3$  mm<sup>3</sup>.

### MPRAGE Processing

Two T1-weighted anatomical images were acquired for each participant and were submitted to the previously described FreeSurfer pipeline (Dale et al., 1999; Fischl et al., 1999). Briefly, the two T1-weighted images were rigid body registered to each other, averaged to increase signal-to-noise (SNR), reoriented into a common space, bias field corrected in which the intensity at each voxel is divided by the estimated bias field at that location, skull stripped using a deformable template model (Segonne et al., 2004), and then tissue classified based on intensity gradients and *a priori* boundaries between white and grey matter regions. Images were then manually edited slice-by-slice for pial surface and cerebellar misclassifications.

### Resting-State Processing

Intrinsic connectivity during resting state fMRI was assessed via independent component analysis using FMRIB's Software Library (FSL) Multivariate Exploratory Linear Optimized Decomposition into Independent Components (MELODIC) tool (<http://fsl.fmrib.ox.ac.uk/fsl/fsl-4.1.9/melodic/index.html>). ICA is a statistical technique that decomposes a summative signal into independent additive spatiotemporal subcomponents. MELODIC's multi-session temporal concatenation option was employed to allow for the identification of group-level spontaneous intrinsic brain networks, or subcomponents. We allowed MELODIC to estimate the optimal number of components across the group.

The resting-state data were brain-extracted (Smith, 2002), motion corrected to the median functional image using b-spline interpolation, temporally filtered with a 100 second high-pass filter, and spatially smoothed with a 7 mm full width at half maximum (FWHM) kernel. The previously skull stripped anatomical volumes (see FreeSurfer steps above) were registered to the standard space T1 MNI  $2 \times 2 \times 2$  mm template with FSL's Non-linear Image Registration Tool (FNIRT; <http://www.fmrib.ox.ac.uk/analysis/techrep>). Each participant's median functional image was then co-registered to their anatomical volume and warped to standard space using the non-linear warping matrix generated during the transformation of the anatomical volume to standard space. All resulting functional images were interpolated to  $2 \times 2 \times 2$  mm resolution for group-level network identification.

The DMN component was identified (component 10), isolated using FSL's *fsl\_roi* command, and thresholded at a significance level of  $Z > 4.3$ . The thresholding yielded a DMN map composed of midline frontal and parietal regions (Figure 1). The ventral medial prefrontal cortex region was predominantly composed of paracingulate and anterior cingulate voxels

(peak;  $x = -4$ ,  $y = 52$ ,  $z = 4$ ) and the parietal region was predominantly composed of the precuneus and posterior cingulate voxels (peak;  $x = -6$ ,  $y = -56$ ,  $z = 20$ ). The thresholded DMN map was then binarized and multiplied by the 2mm Harvard-Oxford Atlas (25% threshold) using FSL's *fslmaths* command in order to create a single DMN ROI mask.

### CBF Processing and Analysis

The initial step in processing the perfusion data was to isolate magnetization recovery image for blood, or  $M_0$ , using FSL's *fslroi* utility (<http://fsl.fmrib.ox.ac.uk/fsl/fslwiki/Fslutils>).  $M_0$  serves as an internal reference to calibrate the perfusion-weighted images to generate absolute CBF (ml/100g/min) maps. Brain masks were next generated from each  $M_0$  image using FSL's brain extraction tool (BET v2.1) and were applied to the remaining tagged and untagged pairs of images in order to exclude non-brain voxels from further consideration. The  $M_0$  image was then registered to the high-resolution T1 anatomical image with an affine transformation with six degrees of freedom using FMRIB's Linear Image Registration Tool (FLIRT; (Jenkinson et al., 2002; Jenkinson and Smith, 2001)). This generated a transformation matrix for the warping of perfusion-weighted images into anatomical space.

Next, a perfusion-weighted image (relative CBF) was created by performing a tag-control subtraction followed by an averaging of the difference images using FSL's *asl\_file* command, a utility that is part of the Bayesian Inference for Arterial Spin Labeling (BASIL) tool (Chappell et al., 2009). BASIL is a toolkit that employs a Bayesian algorithm to fit a standard kinetic curve model (Buxton et al., 1998) to the ASL data. Absolute CBF was calculated using BASIL's *oxford\_asl* command, which applies the kinetic model inversion to all images and calibrates and registers the perfusion-weighted data. This was achieved by defining the sequence inversion time (`--tis = 1.9 s`), bolus duration (`--bolus = 0.7 s`; `--fixbolus`), slice timing difference (`--slidedt = 0.0625`), repetition time for the  $M_0$  calibration image (`--tr = 3.4 s`), and echo time (`--te = 12 ms`). Default T1 (1.3 s) and T1b (1.6 s) values were used since acquisition was at 3T.

The isolated  $M_0$  image was used to quantify absolute units of CBF by first solving for  $M_0$  in CSF voxels, via automatic segmentation of the ventricles, and then determining the equilibrium magnetization of blood. The perfusion-weighted image was then divided by  $M_0$  to yield absolute CBF (ml/100g/min). Individual perfusion calibrated CBF maps were then registered to the high-resolution T1 anatomical image with an affine transformation with six degrees of freedom by referencing the transformation matrix generated from the  $M_0$  to structural space registration (`--asl2struc`). These maps were then warped to standard space using the non-linear warping matrix generated during the transformation of the anatomical volume to standard space (T1 MNI  $2 \times 2 \times 2$  mm template). Fig. 2A and 2C depict the results of a warped CBF map in a single representative subject.

Individual CBF maps were next multiplied by the previously generated DMN masks and thresholded at a value of 15 to reduce partial voluming effects. A value of 15 was selected to prevent the inclusion of grey-white matter boundary voxels with CBF values suggestive of physiological ischemia (Hossmann, 1994), while including voxels with values suggestive of viable cerebral tissue (Ohashi et al., 2005; Powers et al., 1985). Fig. 2B and 2D depict the DMN ROI mask in a single representative subject. Finally, mean CBF values were extracted

from a single DMN ROI, collapsed across medial frontal and parietal regions, using FSL's *fslstat* command.

### Mediation Analysis

An SPSS macro designed to perform a multiple mediator bootstrapping model with bias-corrected confidence estimates was used to explore the mediation effect of fitness<sub>CR</sub> on the relationship between GLS and DMN CBF (Preacher and Hayes, 2004). In addition, an alternative analysis was used to explore the mediation effect of GLS on the relationship between fitness<sub>CR</sub> and DMN CBF. The 95% confidence interval of the indirect effect was obtained with 1000 bootstrap resamples.

### Results

Demographic, fitness<sub>CR</sub>, and GLS data are presented in Table 1. Although this study is not investigating sex differences related to GLS or fitness<sub>CR</sub>, we did observe a significant sex difference for height, weight, GLS, VO<sub>2</sub> peak, and total time on treadmill. Male participants demonstrated significantly higher values for height [ $F(1, 28) = 36.16$  for  $P < 0.0001$ ], weight [ $F(1, 28) = 14.29$  for  $P = 0.001$ ], VO<sub>2</sub> peak [ $F(1, 28) = 15.46$  for  $P = 0.001$ ], and total time on treadmill [ $F(1, 28) = 9.04$  for  $P = 0.006$ ]. In addition, male participants also demonstrated significantly lower GLS values [ $F(1, 28) = 5.81$  for  $P = 0.023$ ] indicating better myocardial mechanical function.

Partial correlations between the independent variables and DMN CBF while controlling for age and sex revealed that GLS demonstrated a significant positive relationship with CBF ( $r = 0.40$ ,  $p = 0.048$ ) and a marginal positive relationship with fitness<sub>CR</sub> ( $r = 0.29$ ,  $p = 0.086$ ). Fitness<sub>CR</sub> showed a significant positive correlation with DMN CBF ( $r = 0.57$ ,  $p = 0.010$ ). Scatter plots illustrating these relationships are presented in Fig. 3.

Multiple regression analyses were conducted to assess each component of the proposed mediation model. First, it was found that GLS was positively associated with DMN CBF (beta = 1.10,  $t(26) = 2.07$ ,  $p = 0.048$ ). A marginal positive relationship was observed between GLS and fitness<sub>CR</sub> (beta = 0.032,  $t(26) = 1.79$ ,  $p = 0.086$ ). Finally, results indicated that the mediator, fitness<sub>CR</sub>, was positively associated with DMN CBF (beta = 14.49,  $t(26) = 2.76$ ,  $p = 0.010$ ). Results of the mediation analysis confirmed the mediating role of fitness<sub>CR</sub> in the relationship between GLS and DMN CBF (beta = 0.46; CI = 0.05 to 1.23). In addition, results indicated that the direct effect of GLS on DMN CBF became non-significant (beta = 0.64,  $t(26) = 1.28$ ,  $p = 0.213$ ). The mediation model illustrating this relationship is presented in Fig. 4. Alternatively, GLS failed to show a mediating role in the relationship between fitness<sub>CR</sub> and DMN CBF (beta = 2.21; CI = -0.08 to 9.01).

Finally, to determine if our findings were specific to regions with high resting metabolic rates we explored relationships between CBF, GLS and fitness<sub>CR</sub> in the task positive network (TPN) and compared the strength of correlations between the TPN and DMN. No significant relationship was observed between TPN CBF and GLS ( $r = 0.18$ ,  $p = 0.39$ ) or TPN CBF and fitness<sub>CR</sub> ( $r = 0.38$ ,  $p = 0.13$ ). Despite a lack of association in the TPN, there was no significant difference in the strength of correlations between DMN CBF and GLS

and TPN CBF and GLS ( $z_{\text{obs}} = 0.89$ ;  $-1.96 > z > 1.96$ ), or between DMN CBF and  $\text{fitness}_{\text{CR}}$  and TPN CBF and  $\text{fitness}_{\text{CR}}$  ( $z_{\text{obs}} = 0.91$ ;  $-1.96 > z > 1.96$ ).

## DISCUSSION

The present study represents the first exploration of relationships between both  $\text{fitness}_{\text{CR}}$  and heart function on brain CBF. Our results build upon findings that both cardiac function and  $\text{fitness}_{\text{CR}}$  help to maintain the structural and functional integrity of the aged brain (Colcombe et al., 2006; Kramer et al., 2005; Zuccala et al., 1997). Specifically we found that GLS, a measure of left ventricular myocardial mechanics, and  $\text{fitness}_{\text{CR}}$  were associated with greater DMN CBF. Moreover, our results showed that  $\text{fitness}_{\text{CR}}$  mediated the relationship between myocardial function and DMN CBF. These findings provide more evidence to support the role that  $\text{fitness}_{\text{CR}}$  plays in the maintenance of cerebral vitality in late adulthood. The findings also highlight the relationship between myocardial function and CBF. The implications of these findings are discussed below.

Age-related decreases in CBF are a common finding in the literature and represent one of many potential mechanisms that contribute to declines in the integrity of the aged brain (Ainslie et al., 2008; Bertsch et al., 2009; Buijs et al., 1998; Tarumi et al., 2014). Age-related changes in GLS have also been reported in the literature (Dalen et al., 2010; Kaku et al., 2014), and appear to be a more sensitive indicator of myocardial dysfunction when compared to ejection fraction (Ersboll et al., 2013; Sjoli et al., 2009). We therefore chose to focus the attention of this study on quantifying both GLS and CBF to the DMN. The DMN was selected because it is comprised of several cortical regions, including the precuneus and cingulate cortex, that show high resting metabolic rates (Buckner et al., 2008; Gusnard and Raichle, 2001) and susceptibility to AD pathophysiology (Braak and Del Tredici, 2011; Buckner et al., 2005). We found that better myocardial function was associated with greater CBF to anterior and posterior portions of the cingulate cortex and precuneus. Our results build on recent findings that GLS is related to cerebrovascular health in individuals with normal left ventricular ejection fraction (Russo et al., 2013).

We also chose to focus our attention on a protective factor related to both heart health and brain health,  $\text{fitness}_{\text{CR}}$ .  $\text{Fitness}_{\text{CR}}$  is a strong marker of health that declines with age (Fleg et al., 2005; Stathokostas et al., 2004) and reduces the risk of both Alzheimer's disease and cardiovascular disease (Bassuk and Manson, 2003; Hamer and Chida, 2009). We opted to use a composite measure of  $\text{fitness}_{\text{CR}}$ , which included  $\text{VO}_2$  peak and total time on treadmill, because we previously observed that these two variables were predictive of WM microstructure (Johnson et al., 2012). Similar to myocardial function, we observed a positive relationship between  $\text{fitness}_{\text{CR}}$  and DMN CBF. Our results provide additional evidence for the supportive nature that  $\text{fitness}_{\text{CR}}$  plays in maintaining brain health.

Since training-induced increases in  $\text{fitness}_{\text{CR}}$  are not associated with augmented cardiac output at rest (Ehsani et al., 1991; Stratton et al., 1994), we determined the indirect effect of GLS, a proxy of cardiac function, on DMN CBF through our mediator variable  $\text{fitness}_{\text{CR}}$ . Results indicated that  $\text{fitness}_{\text{CR}}$  mediated the effects of resting myocardial function on DMN CBF and suggest that the detrimental effects of age-related declines in myocardial function

on brain health are ameliorated by fitness<sub>CR</sub>. Thus, maintaining fitness<sub>CR</sub> through regular physical activity and exercise is instrumental in preserving brain health late in life, as declines in cardiac function are associated with cognitive impairment (Almeida and Tamai, 2001; Vogels et al., 2007; Zuccala et al., 1997). Moreover, low normal measures of resting cardiac function are associated with smaller brain volumes, delayed recall, and poorer cognitive performance (Jefferson et al., 2011; Jefferson et al., 2010).

Individual differences in myocardial function represent a potential mechanism for differences in brain function, but the underlying physiology responsible for this relationship is poorly understood. Previous findings have demonstrated that lower GLS is associated with increased arterial stiffness (Russo et al., 2011) and that increased arterial stiffness reduces CBF (Kielstein et al., 2006). Arterial stiffness increases with age (Mitchell et al., 2004) and may therefore contribute to age-related declines in the structural and functional integrity of the brain (Hanon et al., 2005; Ohmine et al., 2008). However, superior fitness<sub>CR</sub> is associated with reduced arterial stiffness (Vaitkevicius et al., 1993) and may therefore help to explain the mediating role observed in this study. Future longitudinal study designs are needed to determine if improved fitness<sub>CR</sub> results in improved vascular compliance in healthy older adults.

Unlike the DMN, CBF in the task positive network (TPN) was not related to GLS or fitness<sub>CR</sub>. This lack of relationship is not surprising since participants were not actively engaged in a task. However, it should be noted that the CBF-GLS and CBF-fitness<sub>CR</sub> associations within the DMN network were not statistically stronger than those in the TPN. Thus, our results do not permit a conclusion that the effects of our fitness/heart measures on CBF are strongest in the DMN. This question remains a relevant one to be addressed in future studies with larger sample sizes given the tightly regulated relationship between CBF and active cortical regions (van Beek et al., 2008; Wagner et al., 2012) and previously reported relationships between fitness<sub>CR</sub> and functional activity in task dependent cortical regions (Colcombe et al., 2004; Holzsneider et al., 2012).

The present study has a few caveats that open the door for future research. First, the cross-sectional design of our study limits our ability to make causal claims about the relationships between GLS, fitness<sub>CR</sub>, and CBF. However, the relationships reported in this study serve to justify future intervention studies focused on determining if improved fitness<sub>CR</sub> leads to increases in DMN CBF, or improvements in GLS. Second, longitudinal study designs will help to elucidate whether or not improved GLS, fitness<sub>CR</sub>, and DMN CBF yield any cognitive benefit during active task performance. Findings from such studies could potentially help to identify a unifying potential physiological mechanism behind the reduced deactivations seen in the DMN in both normal aging and Alzheimer's disease (Grady et al., 2006; Lustig et al., 2003). Third, our work focused exclusively on the DMN and a single imaging modality, ASL. Future work should adopt multimodal strategies to gain a more complete understanding of the relationship between GLS and other proxies of brain health. For example, future studies should collect fMRI and echocardiography data to determine if improved left ventricular myocardial function results in cognitive gains associated with TPN activity. Moreover, combining fMRI and ASL modalities has been shown to maximize the efficacy of perfusion data by increasing the SNR (Zhu et al., 2013). Finally, although we

encouraged participants to abstain from consuming caffeine and alcohol 24 hours prior to scanning, we acknowledge that compliance to such requests are not guaranteed. Thus, such factors could have contributed to our CBF values (Chen and Parrish, 2009; Gundersen et al., 2013).

In conclusion, our results demonstrate that a clinical measure of myocardial function, GLS, is associated with CBF to the DMN. Moreover, a combined measure of fitness<sub>CR</sub> previously found to be associated with WM integrity demonstrated a positive relationship with CBF to the DMN. Fitness<sub>CR</sub> also mediated the effect of GLS on DMN CBF, suggesting that fitness<sub>CR</sub> late in life may play a significant role in maintaining CBF despite age-related changes in heart health. These findings motivate future longitudinal and multimodal studies aimed at determining if increased levels of physical activity improve measures of left ventricular myocardial mechanics and attenuate age-related declines in CBF and cognition.

## ACKNOWLEDGEMENTS

This study was supported by the National Institutes of Health CTSA UL1TR000117 and the University of Kentucky's Clinical Services Core (CSC). Specifically we would like to thank the Translational Analytics and Assessment Support (TAAS) lab for collecting all fitness-related measures. The content is solely the responsibility of the authors and does not necessarily represent the official views of these granting agencies.

## REFERENCES

1. Ainslie PN, Cotter JD, George KP, Lucas S, Murrell C, Shave R, Thomas KN, Williams MJ, Atkinson G. Elevation in cerebral blood flow velocity with aerobic fitness throughout healthy human ageing. *J Physiol*. 2008; 586:4005–4010. [PubMed: 18635643]
2. Almeida OP, Tamai S. Congestive heart failure and cognitive functioning amongst older adults. *Arq Neuropsiquiatr*. 2001; 59:324–329. [PubMed: 11460173]
3. Bassuk SS, Manson JE. Physical activity and the prevention of cardiovascular disease. *Current atherosclerosis reports*. 2003; 5:299–307. [PubMed: 12793971]
4. Bertsch K, Hagemann D, Hermes M, Walter C, Khan R, Naumann E. Resting cerebral blood flow, attention, and aging. *Brain Res*. 2009; 1267:77–88. [PubMed: 19272361]
5. Braak H, Del Tredici K. Alzheimer's pathogenesis: is there neuron-to-neuron propagation? *Acta neuropathologica*. 2011; 121:589–595. [PubMed: 21516512]
6. Buckner RL, Andrews-Hanna JR, Schacter DL. The brain's default network: anatomy, function, and relevance to disease. *Annals of the New York Academy of Sciences*. 2008; 1124:1–38. [PubMed: 18400922]
7. Buckner RL, Carroll DC. Self-projection and the brain. *Trends in cognitive sciences*. 2007; 11:49–57. [PubMed: 17188554]
8. Buckner RL, Snyder AZ, Shannon BJ, LaRossa G, Sachs R, Fotenos AF, Sheline YI, Klunk WE, Mathis CA, Morris JC, Mintun MA. Molecular, structural, and functional characterization of Alzheimer's disease: evidence for a relationship between default activity, amyloid, and memory. *The Journal of neuroscience : the official journal of the Society for Neuroscience*. 2005; 25:7709–7717. [PubMed: 16120771]
9. Buijjs PC, Krabbe-Hartkamp MJ, Bakker CJ, de Lange EE, Ramos LM, Breteler MM, Mali WP. Effect of age on cerebral blood flow: measurement with ungated two-dimensional phase-contrast MR angiography in 250 adults. *Radiology*. 1998; 209:667–674. [PubMed: 9844657]
10. Buxton RB, Frank LR, Wong EC, Siewert B, Warach S, Edelman RR. A general kinetic model for quantitative perfusion imaging with arterial spin labeling. *Magnetic resonance in medicine : official journal of the Society of Magnetic Resonance in Medicine / Society of Magnetic Resonance in Medicine*. 1998; 40:383–396.

11. Chappell MA, Groves AR, Whitcher B, Woolrich MW. Variational Bayesian Inference for a Nonlinear Forward Model. *Ieee Transactions on Signal Processing*. 2009; 57:223–236.
12. Chen Y, Parrish TB. Caffeine's effects on cerebrovascular reactivity and coupling between cerebral blood flow and oxygen metabolism. *Neuroimage*. 2009; 44:647–652. [PubMed: 19000770]
13. Colcombe SJ, Erickson KI, Scalf PE, Kim JS, Prakash R, McAuley E, Elavsky S, Marquez DX, Hu L, Kramer AF. Aerobic exercise training increases brain volume in aging humans. *J Gerontol A Biol Sci Med Sci*. 2006; 61:1166–1170. [PubMed: 17167157]
14. Colcombe SJ, Kramer AF, Erickson KI, Scalf P, McAuley E, Cohen NJ, Webb A, Jerome GJ, Marquez DX, Elavsky S. Cardiovascular fitness, cortical plasticity, and aging. *Proc Natl Acad Sci U S A*. 2004; 101:3316–3321. [PubMed: 14978288]
15. Dale AM, Fischl B, Sereno MI. Cortical surface-based analysis. I. Segmentation and surface reconstruction. *Neuroimage*. 1999; 9:179–194. [PubMed: 9931268]
16. Dalen H, Thorstensen A, Aase SA, Ingul CB, Torp H, Vatten LJ, Stoylen A. Segmental and global longitudinal strain and strain rate based on echocardiography of 1266 healthy individuals: the HUNT study in Norway. *European journal of echocardiography : the journal of the Working Group on Echocardiography of the European Society of Cardiology*. 2010; 11:176–183.
17. de la Torre JC, Perry G, Maccioni RB. Cerebral and cardiac vascular pathology in Alzheimer's Disease. *Current Hypotheses and Research Milestones in Alzheimer's Disease Springer US*. New York. 2009:159–169.
18. de la Torre JC. The vascular hypothesis of Alzheimer's disease: bench to bedside and beyond. *Neuro-degenerative diseases*. 2010; 7:116–121. [PubMed: 20173340]
19. Dixon ML, Fox KC, Christoff K. A framework for understanding the relationship between externally and internally directed cognition. *Neuropsychologia*. 2014; 62:321–330. [PubMed: 24912071]
20. Ehsani AA, Ogawa T, Miller TR, Spina RJ, Jilka SM. Exercise training improves left ventricular systolic function in older men. *Circulation*. 1991; 83:96–103. [PubMed: 1984902]
21. Ersboll M, Valeur N, Mogensen UM, Andersen MJ, Moller JE, Velazquez EJ, Hassager C, Sogaard P, Kober L. Prediction of all-cause mortality and heart failure admissions from global left ventricular longitudinal strain in patients with acute myocardial infarction and preserved left ventricular ejection fraction. *J Am Coll Cardiol*. 2013; 61:2365–2373. [PubMed: 23563128]
22. Fischl B, Sereno MI, Dale AM. Cortical surface-based analysis. II: Inflation, flattening, and a surface-based coordinate system. *Neuroimage*. 1999; 9:195–207. [PubMed: 9931269]
23. Fleg JL, Morrell CH, Bos AG, Brant LJ, Talbot LA, Wright JG, Lakatta EG. Accelerated longitudinal decline of aerobic capacity in healthy older adults. *Circulation*. 2005; 112:674–682. [PubMed: 16043637]
24. Grady CL, Springer MV, Hongwanishkul D, McIntosh AR, Winocur G. Age-related changes in brain activity across the adult lifespan. *J Cogn Neurosci*. 2006; 18:227–241. [PubMed: 16494683]
25. Gundersen H, van Wageningen H, Gruner R. Alcohol-induced changes in cerebral blood flow and cerebral blood volume in social drinkers. *Alcohol Alcohol*. 2013; 48:160–165. [PubMed: 23171612]
26. Gusnard DA, Raichle ME. Searching for a baseline: functional imaging and the resting human brain. *Nature reviews. Neuroscience*. 2001; 2:685–694. [PubMed: 11584306]
27. Hamer M, Chida Y. Physical activity and risk of neurodegenerative disease: a systematic review of prospective evidence. *Psychol Med*. 2009; 39:3–11. [PubMed: 18570697]
28. Hanon O, Haulon S, Lenoir H, Seux ML, Rigaud AS, Safar M, Girerd X, Forette F. Relationship between arterial stiffness and cognitive function in elderly subjects with complaints of memory loss. *Stroke*. 2005; 36:2193–2197. [PubMed: 16151027]
29. Hoit BD. Strain and strain rate echocardiography and coronary artery disease. *Circulation. Cardiovascular imaging*. 2011; 4:179–190. [PubMed: 21406664]
30. Holzsneider K, Wolbers T, Roder B, Hotting K. Cardiovascular fitness modulates brain activation associated with spatial learning. *Neuroimage*. 2012; 59:3003–3014. [PubMed: 22027496]
31. Hossmann KA. Viability thresholds and the penumbra of focal ischemia. *Ann Neurol*. 1994; 36:557–565. [PubMed: 7944288]

32. Jefferson AL, Himali JJ, Au R, Seshadri S, Decarli C, O'Donnell CJ, Wolf PA, Manning WJ, Beiser AS, Benjamin EJ. Relation of left ventricular ejection fraction to cognitive aging (from the Framingham Heart Study). *The American journal of cardiology*. 2011; 108:1346–1351. [PubMed: 21880293]
33. Jefferson AL, Himali JJ, Beiser AS, Au R, Massaro JM, Seshadri S, Gona P, Salton CJ, DeCarli C, O'Donnell CJ, Benjamin EJ, Wolf PA, Manning WJ. Cardiac index is associated with brain aging: the Framingham Heart Study. *Circulation*. 2010; 122:690–697. [PubMed: 20679552]
34. Jenkinson M, Bannister P, Brady M, Smith S. Improved optimization for the robust and accurate linear registration and motion correction of brain images. *Neuroimage*. 2002; 17:825–841. [PubMed: 12377157]
35. Jenkinson M, Smith S. A global optimisation method for robust affine registration of brain images. *Medical image analysis*. 2001; 5:143–156. [PubMed: 11516708]
36. Johnson NF, Kim C, Clasey JL, Bailey A, Gold BT. Cardiorespiratory fitness is positively correlated with cerebral white matter integrity in healthy seniors. *Neuroimage*. 2012; 59:1514–1523. [PubMed: 21875674]
37. Kaku K, Takeuchi M, Tsang W, Takigiku K, Yasukochi S, Patel AR, Mor-Avi V, Lang RM, Otsuji Y. Age-related normal range of left ventricular strain and torsion using three-dimensional speckle-tracking echocardiography. *Journal of the American Society of Echocardiography : official publication of the American Society of Echocardiography*. 2014; 27:55–64. [PubMed: 24238753]
38. Kielstein JT, Donnerstag F, Gasper S, Menne J, Kielstein A, Martens-Lobenhoffer J, Scalera F, Cooke JP, Fliser D, Bode-Boger SM. ADMA increases arterial stiffness and decreases cerebral blood flow in humans. *Stroke*. 2006; 37:2024–2029. [PubMed: 16809568]
39. Koch W, Teipel S, Mueller S, Buerger K, Bokde AL, Hampel H, Coates U, Reiser M, Meindl T. Effects of aging on default mode network activity in resting state fMRI: does the method of analysis matter? *Neuroimage*. 2010; 51:280–287. [PubMed: 20004726]
40. Kramer AF, Colcombe SJ, McAuley E, Scalf PE, Erickson KI. Fitness, aging and neurocognitive function. *Neurobiol Aging* 26 Suppl. 2005; 1:124–127.
41. Kramer AF, Erickson KI. Capitalizing on cortical plasticity: influence of physical activity on cognition and brain function. *Trends Cogn Sci*. 2007; 11:342–348. [PubMed: 17629545]
42. Lustig C, Snyder AZ, Bhakta M, O'Brien KC, McAvoy M, Raichle ME, Morris JC, Buckner RL. Functional deactivations: change with age and dementia of the Alzheimer type. *Proc Natl Acad Sci U S A*. 2003; 100:14504–14509. [PubMed: 14608034]
43. Mitchell GF, Parise H, Benjamin EJ, Larson MG, Keyes MJ, Vita JA, Vasan RS, Levy D. Changes in arterial stiffness and wave reflection with advancing age in healthy men and women: the Framingham Heart Study. *Hypertension*. 2004; 43:1239–1245. [PubMed: 15123572]
44. Mor-Avi V, Lang RM, Badano LP, Belohlavek M, Cardim NM, Derumeaux G, Galderisi M, Marwick T, Nagueh SF, Sengupta PP, Sicari R, Smiseth OA, Smulevitz B, Takeuchi M, Thomas JD, Vannan M, Voigt JU, Zamorano JL. Current and evolving echocardiographic techniques for the quantitative evaluation of cardiac mechanics: ASE/EAE consensus statement on methodology and indications endorsed by the Japanese Society of Echocardiography. *Journal of the American Society of Echocardiography : official publication of the American Society of Echocardiography*. 2011; 24:277–313. [PubMed: 21338865]
45. Ohashi M, Tsuji A, Kaneko M, Matsuda M. Threshold of regional cerebral blood flow for infarction in patients with acute cerebral ischemia. *J Neuroradiol*. 2005; 32:337–341. [PubMed: 16424835]
46. Ohmine T, Miwa Y, Yao H, Yuzuriha T, Takashima Y, Uchino A, Takahashi-Yanaga F, Morimoto S, Maehara Y, Sasaguri T. Association between arterial stiffness and cerebral white matter lesions in community-dwelling elderly subjects. *Hypertens Res*. 2008; 31:75–81. [PubMed: 18360021]
47. Powers WJ, Grubb RL Jr, Darriet D, Raichle ME. Cerebral blood flow and cerebral metabolic rate of oxygen requirements for cerebral function and viability in humans. *J Cereb Blood Flow Metab*. 1985; 5:600–608. [PubMed: 3877067]
48. Preacher KJ, Hayes AF. SPSS and SAS procedures for estimating indirect effects in simple mediation models. *Behavior Research Methods, Instruments, & Computers: A Journal Of The Psychonomic Society, Inc*. 2004; 36:717–731.

49. Reisner SA, Lysyansky P, Agmon Y, Mutlak D, Lessick J, Friedman Z. Global longitudinal strain: a novel index of left ventricular systolic function. *Journal of the American Society of Echocardiography : official publication of the American Society of Echocardiography*. 2004; 17:630–633. [PubMed: 15163933]
50. Russo C, Jin Z, Homma S, Elkind MS, Rundek T, Yoshita M, DeCarli C, Wright CB, Sacco RL, Di Tullio MR. Subclinical left ventricular dysfunction and silent cerebrovascular disease: the Cardiovascular Abnormalities and Brain Lesions (CABL) study. *Circulation*. 2013; 128:1105–1111. [PubMed: 23902759]
51. Russo C, Jin Z, Takei Y, Hasegawa T, Koshaka S, Palmieri V, Elkind MS, Homma S, Sacco RL, Di Tullio MR. Arterial wave reflection and subclinical left ventricular systolic dysfunction. *Journal of hypertension*. 2011; 29:574–582. [PubMed: 21169863]
52. Segonne F, Dale AM, Busa E, Glessner M, Salat D, Hahn HK, Fischl B. A hybrid approach to the skull stripping problem in MRI. *Neuroimage*. 2004; 22:1060–1075. [PubMed: 15219578]
53. Sjolli B, Orn S, Grenne B, Vartdal T, Smiseth OA, Edvardsen T, Brunvand H. Comparison of left ventricular ejection fraction and left ventricular global strain as determinants of infarct size in patients with acute myocardial infarction. *Journal of the American Society of Echocardiography : official publication of the American Society of Echocardiography*. 2009; 22:1232–1238. [PubMed: 19815383]
54. Smith PJ, Blumenthal JA, Hoffman BM, Cooper H, Strauman TA, Welsh-Bohmer K, Browndyke JN, Sherwood A. Aerobic exercise and neurocognitive performance: a meta-analytic review of randomized controlled trials. *Psychosomatic medicine*. 2010; 72:239–252. [PubMed: 20223924]
55. Smith SM. Fast robust automated brain extraction. *Human brain mapping*. 2002; 17:143–155. [PubMed: 12391568]
56. Stathokostas L, Jacob-Johnson S, Petrella RJ, Paterson DH. Longitudinal changes in aerobic power in older men and women. *J Appl Physiol*. 2004; 97:781–789. [PubMed: 15047671]
57. Stratton JR, Levy WC, Cerqueira MD, Schwartz RS, Abrass IB. Cardiovascular responses to exercise. Effects of aging and exercise training in healthy men. *Circulation*. 1994; 89:1648–1655. [PubMed: 8149532]
58. Swain RA, Harris AB, Wiener EC, Dutka MV, Morris HD, Theien BE, Konda S, Engberg K, Lauterbur PC, Greenough WT. Prolonged exercise induces angiogenesis and increases cerebral blood volume in primary motor cortex of the rat. *Neuroscience*. 2003; 117:1037–1046. [PubMed: 12654355]
59. Tarumi T, Ayaz Khan M, Liu J, Tseng BY, Parker R, Riley J, Tinajero C, Zhang R. Cerebral hemodynamics in normal aging: central artery stiffness, wave reflection, and pressure pulsatility. *Journal of cerebral blood flow and metabolism : official journal of the International Society of Cerebral Blood Flow and Metabolism*. 2014; 34:1255.
60. Thompson, WR.; Gordon, NF.; Pescatello, LS., editors. *American College of Sports Medicine's Guidelines for Exercise Testing and Prescription*. 8th ed.. Lippincott Williams and Wilkins; Philadelphia: 2010.
61. Vaitkevicius PV, Fleg JL, Engel JH, O'Connor FC, Wright JG, Lakatta LE, Yin FC, Lakatta EG. Effects of age and aerobic capacity on arterial stiffness in healthy adults. *Circulation*. 1993; 88:1456–1462. [PubMed: 8403292]
62. van Beek AH, Claassen JA, Rikkert MG, Jansen RW. Cerebral autoregulation: an overview of current concepts and methodology with special focus on the elderly. *J Cereb Blood Flow Metab*. 2008; 28:1071–1085. [PubMed: 18349877]
63. Vogels RL, Scheltens P, Schroeder-Tanka JM, Weinstein HC. Cognitive impairment in heart failure: a systematic review of the literature. *European journal of heart failure*. 2007; 9:440–449. [PubMed: 17174152]
64. Wagner M, Jurcoane A, Volz S, Magerkurth J, Zanella FE, Neumann-Haefelin T, Deichmann R, Singer OC, Hattingen E. Age-related changes of cerebral autoregulation: new insights with quantitative T2\*-mapping and pulsed arterial spin-labeling MR imaging. *AJNR. American journal of neuroradiology*. 2012; 33:2081–2087. [PubMed: 22700750]
65. Zhu S, Fang Z, Hu S, Wang Z, Rao H. Resting state brain function analysis using concurrent BOLD in ASL perfusion fMRI. *PLoS one*. 2013; 8:e65884. [PubMed: 23750275]

66. Zuccala G, Cattel C, Manes-Gravina E, Di Niro MG, Cocchi A, Bernabei R. Left ventricular dysfunction: a clue to cognitive impairment in older patients with heart failure. *J Neurol Neurosurg Psychiatry*. 1997; 63:509–512. [PubMed: 9343133]

Author Manuscript

Author Manuscript

Author Manuscript

Author Manuscript

**HIGHLIGHTS**

- Cardiorespiratory fitness is correlated with default mode network blood flow
- Myocardial function is correlated with default mode network blood flow
- Fitness mediates the relationship between myocardial function and blood flow
- Benefits of healthy heart function to brain function are modified by fitness

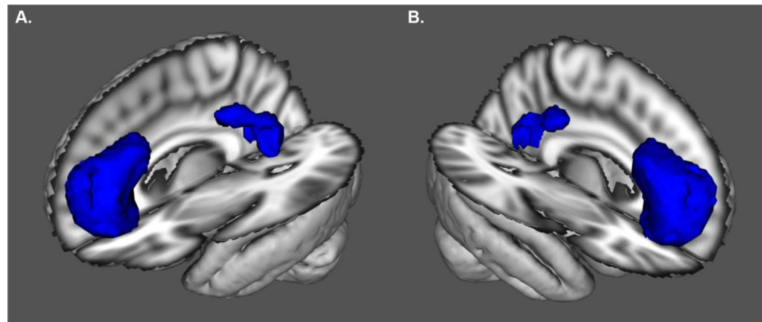


**Figure 1. Default Mode Network Region of Interest**

Anterolateral view of the left (A) and right (B) default mode network (DMN) region of interest (ROI). The ROI was composed of the ventral medial prefrontal cortex and posterior cingulate/precuneus. The DMN ROI was identified using an Independent Component Analysis (ICA). Cerebral blood flow (CBF) was quantified within this ROI using arterial spinal labeling (ASL) MRI. The underlay represents the 3D reconstruction of the MNI152 T1-weighted 2 mm brain.

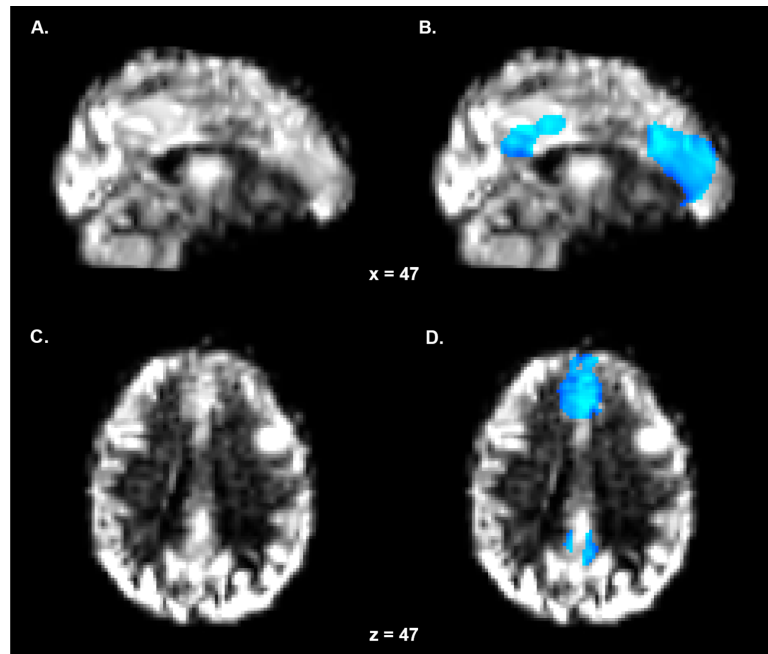


**Figure 2. Perfusion Map and DMN Region of Interest Mask**

(A) Sagittal and (C) axial perfusion calibrated cerebral blood flow (CBF) maps of a single representative subject. The CBF maps were warped to standard space using the non-linear matrix generated during the transformation of the anatomical volume to standard space. (B) Sagittal and (D) axial representations of the DMN region of interest mask overlaid on top of the CBF map. The mask is scaled to CBF (blue-light blue) and thresholded at 15.

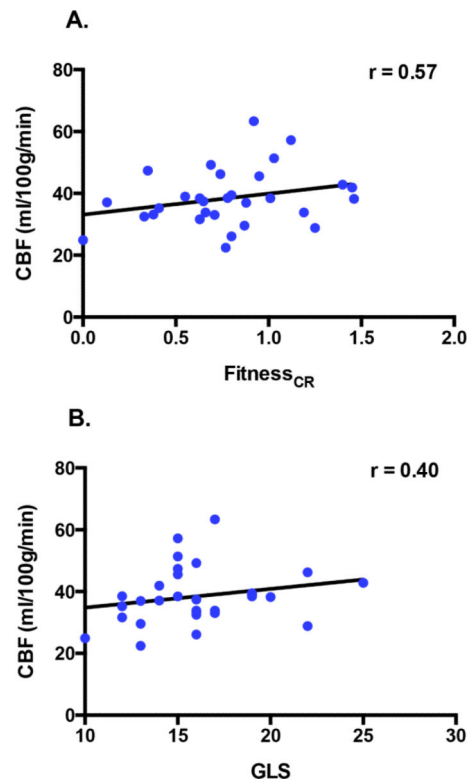


**Figure 3. GLS and Fitness are correlated with DMN CBF**

Scatterplots show relationships between DMN CBF and each health metric.

Cardiorespiratory fitness (fitness<sub>CR</sub>) showed a positive relationship with DMN CBF (A) and GLS showed a positive relationship with DMN CBF (B). Note: To render GLS-CBF relationships more interpretable, participant's GLS values were converted such that higher scores now reflected superior myocardial shortening mechanics (by multiplying each participant's score by  $-1$ ).

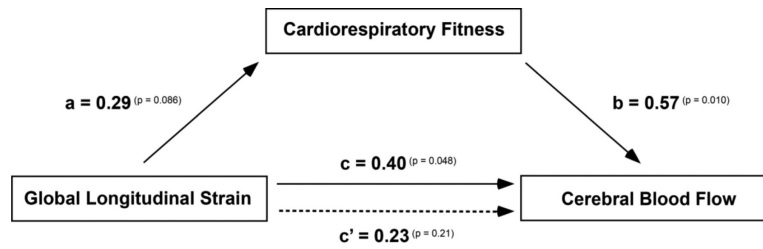


**Figure 4. Mediation Model**

After controlling for age and sex global longitudinal strain (GLS) showed a positive relationship with DMN CBF (path c; solid arrow) and a marginal positive relationship with cardiorespiratory fitness (path a). Cardiorespiratory fitness showed a positive relationship with DMN CBF (path b) and mediated the relationship between GLS and DMN CBF (c'; dashed arrow). Correlations coefficients are depicted with p-value superscripts for each path. Note: To render GLS-CBF relationships more interpretable, participant's GLS values were converted such that higher scores now reflected superior myocardial shortening mechanics (by multiplying each score by  $-1$ ).

**Table 1**

Demographic data, GLS, and fitness test scores.

Subjects	Age	Height (m)	Weight (kg)	GLS (%)	VO <sub>2</sub> Peak (ml/kg/min)	Time On Treadmill (sec)
n = 30	63.7 (2.8)	1.68 (0.11)	70.3 (12.1)	16.0 (3.3)	32.7 (9.0)	1113.5 (190.8)
Female n = 21	63.9 (2.8)	1.63 (0.07)	65.8 (9.39)	15.1 (2.7)	29.2 (6.4)	1052.8 (178.4)
Male n = 9	63.2 (3.0)	1.80 <sup>***</sup> (0.08)	80.9 <sup>*</sup> (11.4)	18.1 (3.8)	40.7 <sup>***</sup> (9.1)	1255.0 <sup>***</sup> (142.0)

Abbreviations: m = meters; kg = kilograms; ml = milliliters; min = minute; s = seconds. GLS values were converted (multiplied by  $-1$ ) such that higher scores reflect superior myocardial shortening mechanics. Note: values are means and values in parentheses are S.D.

<sup>†</sup> $P = 0.010$

<sup>\*\*</sup> $P < 0.005$

<sup>\*</sup> $P = 0.019$

<sup>\*\*\*</sup> $P < 0.0005$ .